International Journal on Magnetic Particle Imaging
Vol 6, No 2, Suppl 1, Article ID 2009015, 3 Pages

Infinite Science Publishing

Proceedings Article

Spatial selectivity enhancement in RF-hyperthermia by magnetic flux confinement

K. Sajjamark[1,*]· H. Lehr[1]· P. Rainer[2]· N. Volker[2]· J. Franke[1]

[1]Bruker BioSpin MRI GmbH, Ettlingen, Germany
[2]Bruker BioSpin GmbH, Rheinstetten, Germany
*Corresponding author, email: kulthisa.sajjamark@bruker.com

Abstract

Aiming to increase spatial selectivity which provides the precision in hyperthermia therapy and high resolution in imaging, we propose a strategy to increase the field gradient for Magnetic Particle Imaging (MPI) modality. In this study, a solution for an existing MPI system topology was simulated, which uses additional soft magnetic material as iron core retrofit at the center of selection field coil. Due to the core property of high magnetic permeability relative to air, the magnetic flux gets confined to increase the selection field gradient field slope. Within this simulation study, the optimal core position is evaluated whilst its effects on the magnet system is validated. We found that this technique increases the magnetic field gradient up to a factor of 1.4 from 2.5 T/m to 3.4 T/m in z-direction, without significant loading of the drive field resonance circuit due to power losses caused by eddy currents in the MPI compatible iron core shielding.

I Introduction

MPI is a new tomographic imaging method which exploits the behavior of superparamagnetic iron-oxide nanoparticles. External magnetic alternating fields are applied to these tracers, while their non-linear response get spatially encoded by a magnetic field gradient [1], featuring a field-free-region. The magnetic field encoding mechanism can be exploited for spatially encoded radio-frequency (RF) hyperthermia [2]. Both techniques, imaging and therapy, can be combined into one theranostic system allowing for in situ therapy [3] [10] and image guided temperature monitoring [4]. It was shown in [1], that an increased selection field gradient leads to higher image resolution capabilities. In hyperthermia therapy, an increased spatial selectivity can minimize thermal damage in healthy tissue. Equivalently to [1] the spatial selectivity is dependent on both the therapy tracer properties as well as the selection field gradient slope [2]. For enlarged FOV (Field of View) in imaging or enlarged FOT (Field of Therapy) in RF-hyperthermia, homogeneous shift or focus fields can be used to superimpose quasi-static homogeneous magnetic offset fields. In RF-hyperthermia, the quasi-static offset fields allow to shift the FOT from the magnetic center of the respective magnet system.

Ferromagnetic core placement is a typical way to confine and enhance magnetic fields [9]. Since a piece of magnetic material is inserted at the coil center, the density of the magnetic flux through the core is confined. The performance of the core depends on the magnetic permeability of the material.

10.18416/ijmpi.2020.2009015

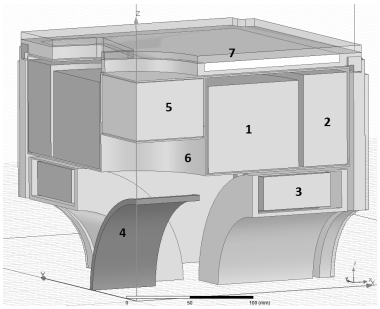

Figure 1: Schematic one-eighth model of the MPI scanner illustrates 1. SF-coil 2. FFz-coil 3. FFx-coil 4. DFx-coil 5. Soft iron core 6. Copper shields and 7. Permenorm shield.

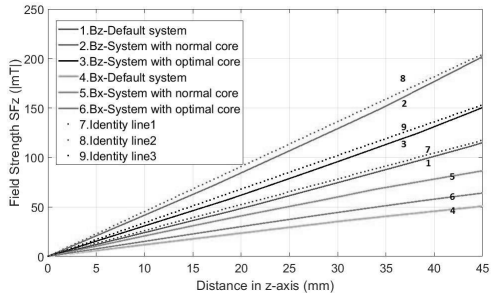

Figure 2: Simulation of SF gradient along x and z-axis.

II Material and methods

A CAD model of a preclinical MPI system (Bruker BioSpin MRI GmbH) with a cylindrical bore and field-free-point (FFP) gradient topology was generated to perform the electromagnetic simulations in ANSYS Maxwell (ANSYS, Inc., Canonsburg, Pennsylvania, U.S.A).

II.I Simulation setting

As shown in Fig. 1, the 7-channel MPI scanner, consisting of Selection Field (SF) coils, 3-axis Focus Field (FF) coils and 3-axis Drive Field (DF) coils, was augmented by a copper shielded soft magnetic iron core with a relative permeability of 64000. Material properties (permeability, conductivity, and coercivity) including the environments of all coils producing magnetic fields were implemented into the model. Due to coil topology symmetry, the field components of y-axis was not simulated as it can be predicted by the fields of x-axis. The maximum currents used in this simulation was 500 A_{DC}, 150 A_{DC} and 150A_{AC} for SF, FF, and DF, respectively. The DF-coil with field direction into the x-axis was simulated with the frequency of 25 kHz which generated the maximum field amplitude of 20 mT.

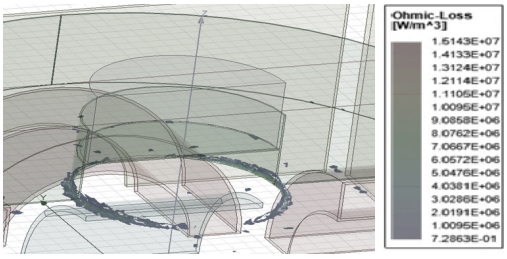

Figure 3: Distribution of power dissipation induced by eddy current of the DFx excitation in the optimal-modified system.

II.II Parameters simulation

We varied the position of the core along z-axis and considered behaviors of the following parameters:

1. Slope of field gradient which is expressed by:

$$G = \frac{|A-B|}{2\cdot 10\text{mm}}, \tag{1}$$

where Gradient slope G is calculated by using field strength at z=±10 mm (A,B).

2. Linearity error L of the field gradient which is determined by:

$$L = 100\left(\frac{|C-D|}{G\cdot 2\cdot 45\text{mm}} - 1\right), \tag{2}$$

using field strength at z=±45 mm (C,D).

3. Ohmic (or power) loss caused by DF-induced eddy-currents in conductive surfaces.
4. Force onto the inserted core.
5. Field amplitudes of FF-coils.
6. FF-homogeneity deviations ΔB which can be expressed by:

$$\Delta B = 100\left(\frac{|E+F|}{2H} - 1\right), \tag{3}$$

where E,F,H corresponds to the field strength at z=±50 mm and z=0 mm, respectively.

7. Maximum FFP offset (Δi) which can be determined by FF amplitude (A_i) and the gradient slope (G_i) at the specific axis (i =x,y,or z):

$$\Delta i = A_i / G_i\,. \tag{4}$$

III Results and discussion

The iron core was placed at the center of SF-coil with the same level as the SF-coil. The field gradient in z-axis, shown in Fig. 2, was boosted up with the factor of 1.6 from 2.5 T/m of the standard scanner to 4.2 T/m of the modified scanner. However, by taking the additional conductive surfaces of the core into account, the

Table 1: Maximum FFP offset capability in x,y,z directions calculated by (4) for standard and modified magnet systems.

	Standard	Modified
max G_z (T/m)	2.5	3.4
$A_{x,y}$, A_z (mT)	18, 45	18.2, 60
Δxy, Δz (mm)	14.4, 18	10.7, 17.5

DF amplitude was damped by eddy current effects by 4 mT. Since DF amplitude damping by core insertion was not desired, the iron core and its copper shield was relocate away from the DF-coil until 20 mT field strength was recovered. This position is called henceforward "optimal position".

The field gradient slope (1) was increased by up to 1.4 times from 2.5 T/m of the conventional scanner to 3.4 T/m of the scanner with optimal core position. The gradient linearity error (2) was 7.5 % which is slightly increased when compared to the system without iron core (7.4 %). Comparing the maximum FFz amplitude of 60 mT for the system with optimal core position and 45 mT for the existing system, the maximum FFP offsets (4) are 17.5 and 18 mm while FFz homogeneity error (4) are 10 % and 17 %, respectively. The field amplitude and homogeneity of the FFx and FFy was not affected significantly by the iron core, as expected. The maximal FFP offset by the FF-coils at the maximal gradients of 2.5 T/m for standard and 3.4 T/m for our modified system are shown below.

The resulting forces onto the inserted core show that SF coil generates 450 N with outward direction from the core and FFz-coils generate ±100 N and force by FFx-coil is neglectable. After we included the magnetic core, our result shows that eddy currents are distributed on the copper screen of the SF-coil as well as the iron core shield. We also investigated the DF induced power dissipation in the copper surfaces, as shown in Fig. 3. The DF losses mostly locates at the edge of copper shield of the SF-coil. Although, iron core causes loss on the system, the overall DF-induced power loss on copper structures was reduced from 101.3 W to 70.2 W for the default system and the system with core, respectively, due to this aforementioned eddy current density distribution.

IV Conclusions

This research presents a simulation study of MPI scanner modification to increase the performance of RF-hyperthermia and imaging by including an additional soft magnetic iron core. The increased gradient, with a factor of 1.4, provides almost 29 % reduction of targeting lesion in hyperthermia [2]. An increased gradient from 2.5 to 3.4 T/m can lead to 25 % improvement of image resolution in MPI imaging, when considering particle sizes of 30 nm[1].

Inserting magnetic material is an affordable and practical method to increase the SF gradient without the need for increased power consumption. Furthermore, this technique allows for an easy upgrade of existing magnet systems. The core localization influences significantly the performance of the magnet system of selection, and focus field mostly in z-axis. In this study, the core position was optimized to compromise the gain of the increased gradient slope and DF induced energy loss. In the future, our experiment with real MPI scanner will be set up to validate the therapeutic selectivity enhancement, by the proposed insertion of soft magnetic material, and the effect on time response of different coils, as in alternating-current devices, the changing magnetic field causes frequency-dependent energy loss [8].

Author's Statement

Acknowledgement of research funding: The work is a part of "Functional Magneto-Therapy" project which is funded by the German Federal Ministry of Education and Research (BMBF, grant number 13GW0230C).

References

[1] J. Rahmer et al. Signal encoding in magnetic particle imaging: properties of the system function, Medical Imaging, vol. 9(4), 2009.

[2] Z. W. Tay et al. Magnetic Particle Imaging Guided Heating In Vivo using Gradient Fields For Arbitrary Localization of Magnetic Hyperthermia Therapy, ACS Nano, vol.12(4), 2018, pp. 3699-3713.

[3] A. Malhotra et al. Tracking the Growth of Superparamagnetic Nanoparticles with an In-Situ Magnetic Particle Spectrometer (INSPECT), Scientific Reports, vol. 9(10538), 2019.

[4] C. Stehning et al. Simultaneous magnetic particle imaging (MPI) and temperature mapping using multi-color MPI, International Journal on MPI, vol.2(2), 2016.

[5] B. Gleich et al. Fast MPI Demonstrator with Enlarged Field of View, Proceedings of ISMRM, vol.18(218), 2010.

[6] T.M. Buzug et al. Magnetic Particle Imaging: Introduction to imaging and hardware realization, Z. Med. Phys., vol. 22(4),2012.

[7] J. Weizenecker et al. A simulation study on the resolution and sensitivity of MPI, Phys. Med. Biol., vol.52, 2007, pp. 6363-6374.

[8] A. Moses et al. Electrical Steels Fundamentals and basic concepts, 1st ed. vol. 1, IET publisher , NJ, 2019, pp. 141-170.

[9] A. Behrends et al. A self-compensating coil setup for combined MPI and magnetic fluid hyperthermia, IWMPI, 2019.

